An Adaptive Nulling Antenna for Military Satellite Communications

William C. Cummings

■ **Using adaptive nulling, an antenna system can reconfigure the receive antenna to produce nulls at the locations of any interference sources. Typically, two generic types of adaptive nulling antennas are considered: the thinned phased array and the multiple-beam antenna. The thinned phased array has excellent nulling resolution but is not a good candidate for area coverage. The multiple-beam antenna, on the other hand, can provide good area coverage but has poorer nulling resolution.**

Lincoln Laboratory has constructed and demonstrated an antenna system that combines the desirable qualities of both types of antennas with the added advantages of multiple simultaneous beam service and extremely light weight. Designed to withstand the rigors of both a launch and a space environment, the antenna produces three simultaneous electronically agile beams, any one of which can be used for area coverage. The antenna operates in the 43.5-to-45.5-GHz band and is capable of producing broadband nulls at least 30 dB deep with a resolution of about 0.1°. Weighing slightly less than 56 lb, the antenna is a viable candidate for military satellite communications.

DURING THE TWENTIETH CENTURY the world has become increasingly dependent on electromagnetic systems. Satellites orbiting the earth provide communications links vital to commerce and government. Radar systems help to navigate aircraft and ships as well as to control the traffic of these vehicles in very crowded skies and harbors. In wartime, the effective coordination and control of land, sea, and air forces require reliable communications. Radar systems are used to locate and track enemy forces, guide friendly forces to their targets, and direct shell and missile fire.

Radio communications systems, radar systems, and, for that matter, any systems that depend on the reception of electromagnetic waves are susceptible to interference, either accidental or deliberate. Over the years a growing number of systems have come into existence and the available radio spectrum has become increasingly crowded. Consequently, the potential for accidental interference has grown to the point that today most systems have experienced interference at least once and many operate in a continuous environment of interference. In wartime, communications and radar systems are subject to both accidental interference resulting from the general confusion of war and deliberate interference by enemy jammers attempting to disrupt and hamper operations.

To combat interference and jamming, system designers often add antijam modulation and coding to improve system performance. Such measures, however, usually increase the width of the frequency band a system must use. Because most systems are required to operate within allocated bandwidths, there is, for this reason if not others, a limit to the interference

protection that coding and antijam modulation can provide.

Because interferors or jammers are usually not co-located with a system's receiver, interference rejection can also be accomplished by tailoring the receiver's antenna pattern to place gain minima or nulls in the directions of the interference sources. If the locations of the interferors are known *a priori*, the receive antenna can be designed with minima in the appropriate directions. Interferor locations, however, are generally not known *a priori*. Interferors come and go, and they can be situated in almost any direction relative to the receive antenna. Thus the receive antenna must be capable of adapting to a changing interference environment.

Properly designed adaptive nulling systems, operating autonomously, can recognize the presence of interfering signals and reconfigure the receive antenna to achieve interference rejection of several tens of decibels in a fraction of a second. The following sections discuss some of the issues involved in the development of adaptive nulling systems and describe a unique lightweight adaptive nulling antenna recently developed at Lincoln Laboratory for use with satellite communications systems.

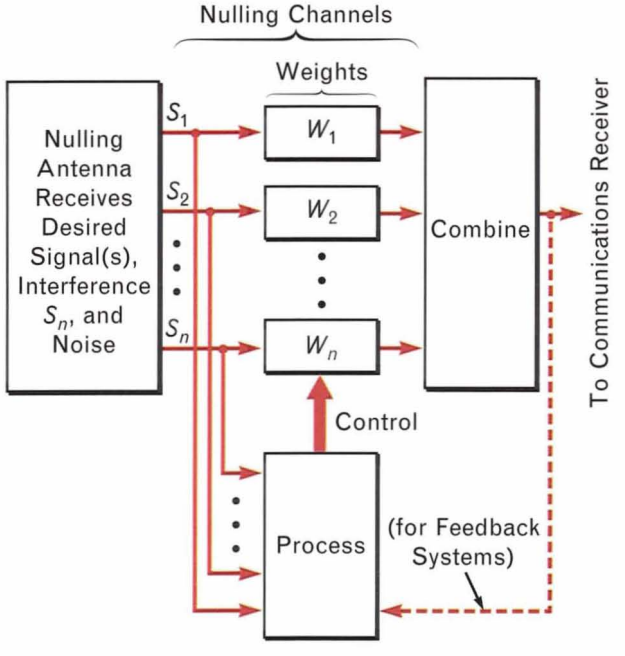

FIGURE 1. Basic nulling circuit. The nulling antenna consists of an array of sensors with outputs containing the desired signal(s), interference, and noise. The processor uses a sampling of each sensor output (and, in the case of feedback systems, the nulling-circuit output is used as well) to determine the weight settings that will result in cancellation of the interference signals in the combiner without seriously affecting the desired signal(s).

Fundamental Principles

Nulling systems require the interfering signals to be received by at least two sensors. The sensors can be the individual antenna elements in an array, the receive ports of a multiple-beam antenna, or just the signals received by separate and not necessarily similar antennas. A nulling system appropriately weighs, in amplitude and phase, each of the signals received by each of the sensors and then combines the weighted signals into a single receiver input such that the interfering signals add destructively and little or no interference is actually received. In effect this process produces nulls oriented in the directions of the interference sources in the composite receive pattern of the sensors.

Figure 1 is a block diagram that illustrates the essentials of a nulling system. The signals received by each sensor consist of the desired receive signal, the interfering signals, and noise. These signals are weighted in amplitude and phase and then summed to produce an output signal that is applied to the input of the receiver. The system determines the weights in accordance with a computational algorithm that seeks to minimize the interference power entering the receiver in accordance with some sort of performance measure and any constraints the system designers may have placed on the nulling system.

Some nulling algorithms require samples only of the signals received by each sensor of the nulling system (such algorithms can be characterized as feedforward). Other algorithms also require a sample of the signal that is applied to the receiver input (such algorithms can be characterized as feedback). The dashed line in Figure 1 shows the connection between the nulling-system output and the nulling-system signal processor required for feedback systems.

Figure 2 is a functional diagram of a two-channel modified Howells-Applebaum nulling system [1]. The heavy lines represent the two signal channels and the shaded rectangle indicates the nulling system's signal

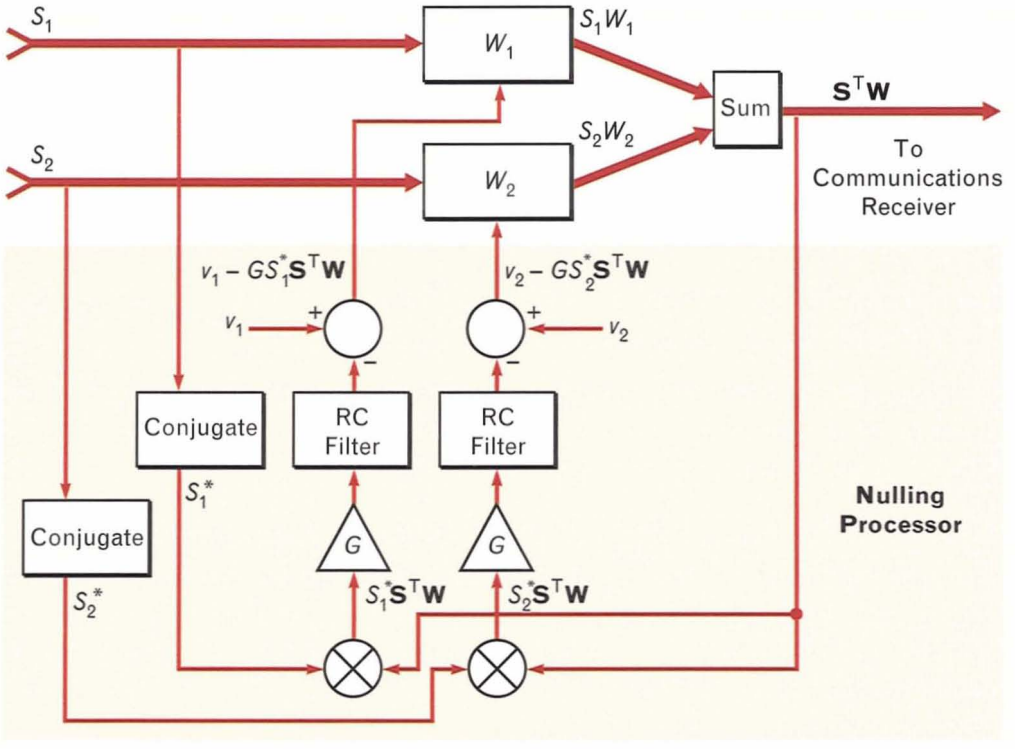

FIGURE 2. Two-channel modified Howells-Applebaum nulling system. Two sensors are shown with interference-signal outputs S_1 and S_2. The two signals are weighted and summed to produce a single output $\mathbf{S}^T\mathbf{W}$, which is applied to the receiver. The nulling processor (indicated by the shaded rectangle) correlates $\mathbf{S}^T\mathbf{W}$ with S_1^* and S_2^*, the conjugate of each of the sensor outputs. The correlation signals are amplified and filtered before being subtracted from the *desired* weight values v_1 and v_2 (i.e., the weight values that would have been used had no interfering signals been present). This process creates control signals that adjust the weights so that the correlator output signal $\mathbf{S}^T\mathbf{W}$ is driven toward zero. Note: $(\,)^*$ indicates conjugate value and $(\,)^T$ indicates matrix transpose.

processor. The received interference signals S_1 and S_2 are multiplied by the nulling weights W_1 and W_2 before being summed and applied to the receiver input. (For simplicity, only S_1 and S_2 are considered, and the desired signal and noise have been omitted from this discussion.) The feedback nulling algorithm determines the appropriate weight values by correlating each of the signals with the receiver input signal and subtracting the result from the *desired* weight values (i.e., those weight values, as determined by the system operator, which would be used if no interfering signals were present). Often the desired weight values are those which would result in the sensor array forming a receive beam pointed in the direction of the desired signal. The low-pass filters (assumed to be RC filters with time constant τ) control the response of the system to the sudden appearance of interference.

The differential equation that describes the system response is

$$\tau \frac{d\mathbf{W}}{dt} + \mathbf{W} = \mathbf{v} - G\left(\mathrm{E}\left[\mathbf{S}^*\mathbf{S}^T\mathbf{W}\right]\right), \qquad (1)$$

where $\mathbf{W}$ is a column vector with entries W_1 and W_2, $\mathbf{v}$ is a column vector with the desired weight entries v_1 and v_2, G is the amplifier gain, $\mathbf{S}$ is a column vector with entries S_1 and S_2, $(\,)^*$ indicates conjugate value, $(\,)^T$ indicates matrix transpose, and E[ ] indicates expected value.

The last term in Equation 1 can be rewritten as

$$G\left(\mathrm{E}\left[\mathbf{S}^*\mathbf{S}^T\mathbf{W}\right]\right) = G\left(\mathrm{E}\left[\mathbf{S}^*\mathbf{S}^T\right]\right)\mathbf{W} = G\mathbf{R}\mathbf{W},$$

where $\mathbf{R}$ is the interference-signal covariance matrix. The steady-state solution to Equation 1 can be de-

termined by setting $\frac{d\mathbf{W}}{dt}$ equal to zero, and solving for $\mathbf{W}$:

$$\mathbf{W} = \left[G\mathbf{R} + \mathbf{I}\right]^{-1}\mathbf{v}, \tag{2}$$

where $\mathbf{I}$ is the identity matrix.

The matrix $[G\mathbf{R} + \mathbf{I}]$ is a positive definite Hermitian matrix and can be written as

$$G\mathbf{R} + \mathbf{I} = \mathbf{U}\Lambda\mathbf{U}^{\mathrm{H}}, \tag{3}$$

where $\mathbf{U}$ is a matrix with columns that are the eigenvectors of $[G\mathbf{R} + \mathbf{I}]$, Λ is a diagonal matrix with entries that are the eigenvalues of $[G\mathbf{R} + \mathbf{I}]$, and $(\,)^{\mathrm{H}}$ indicates conjugate transpose. Thus $\mathbf{W}$ can be written as

$$\mathbf{W} = \mathbf{U}\Lambda^{-1}\mathbf{U}^{\mathrm{H}}\mathbf{v}, \tag{4}$$

where Λ^{-1} is a diagonal matrix with entries that are the reciprocals of the eigenvalues of $[G\mathbf{R} + \mathbf{I}]$.

Although the preceding has described a particular nulling-system concept, most nulling systems will produce adapted weights that can be determined by using expressions similar to that of Equation 4. The adapted weights of virtually all nulling systems depend heavily on the eigenstructure of the interference covariance matrix.

It is possible to obtain some insight into the operation of the nulling system by considering simple examples that do not require detailed mathematical derivations. Consider first a scenario that includes only a single powerful interference source operating within a narrow frequency band. Under these circumstances, and with the assumption that the system noise power is negligible, the matrix Λ will contain a single large eigenvalue $G\lambda$ with the remaining diagonal entries equal to unity. The large eigenvalue is representative of the total interference power received by the nulling antenna. If the nulling antenna has five receiving elements, the matrix takes the form

$$\Lambda = \begin{matrix} G\lambda & 0 & 0 & 0 & 0 \\ 0 & 1 & 0 & 0 & 0 \\ 0 & 0 & 1 & 0 & 0 \\ 0 & 0 & 0 & 1 & 0 \\ 0 & 0 & 0 & 0 & 1 \end{matrix}.$$

The eigenvector associated with the eigenvalue $G\lambda$ can be viewed as a weight vector that directs a maximum-gain antenna beam in the direction of the interferor, and the quiescent weight vector $\mathbf{v}$ can be considered as the weighted sum of the eigenvectors of the covariance matrix; i.e.,

$$\mathbf{v} = a\mathbf{u}_1 + b\mathbf{u}_2 + c\mathbf{u}_3 + d\mathbf{u}_4 + e\mathbf{u}_5. \tag{5}$$

The values of the coefficients *a, b, c, d,* and *e* can be derived easily but are not important to this discussion. The orthonormal nature of the eigenvectors $\mathbf{u}_n$ is such that interference power is coupled into the system via the eigenvector that represents a maximum gain beam in the direction of the interferor. With the assumption that this eigenvector is $\mathbf{u}_1$, the received interference power prior to adaption is

$$\begin{aligned} P_{\text{unadapted}} &= \mathrm{E}\left[\left(\mathbf{S}^{\mathrm{T}}\mathbf{v}\right)^{*}\left(\mathbf{S}^{\mathrm{T}}\mathbf{v}\right)\right] \\ &= \mathbf{v}^{\mathrm{H}}\mathrm{E}\left[\mathbf{S}^{*}\mathbf{S}^{\mathrm{T}}\right]\mathbf{v} \\ &= \mathbf{v}^{\mathrm{H}}\mathbf{R}\mathbf{v}. \end{aligned} \tag{6}$$

From Equation 3

$$\mathbf{R} = \frac{1}{G}\left[\mathbf{U}\Lambda\mathbf{U}^{\mathrm{H}} - \mathbf{I}\right]. \tag{7}$$

Substituting Equations 5 and 7 into Equation 6 results in

$$P_{\text{unadapted}} = aa^{*}\left(\lambda - \frac{1}{G}\right). \tag{8}$$

The adapted weight vector is determined by substituting Equation 5 into 4:

$$\mathbf{W} = a(G\lambda)^{-1}\mathbf{u}_1 + b\mathbf{u}_2 + c\mathbf{u}_3 + d\mathbf{u}_4 + e\mathbf{u}_5, \tag{9}$$

and the received interference power after adaption is given by

$$\begin{aligned} P_{\text{adapted}} &= \mathrm{E}\left[\left(\mathbf{S}^{\mathrm{T}}\mathbf{W}\right)^{*}\left(\mathbf{S}^{\mathrm{T}}\mathbf{W}\right)\right] \\ &= \mathbf{W}^{\mathrm{H}}\mathbf{R}\mathbf{W}. \end{aligned} \tag{10}$$

Substituting Equations 9 and 7 into Equation 10 results in

$$P_{\text{adapted}} = aa^*\left(\lambda - \frac{1}{G}\right)(G\lambda)^{-2}. \qquad (11)$$

Equations 8 and 11 illustrate that the unadapted received interference is proportional to the strength of the interference source and the adapted received interference is approximately proportional to the inverse of the strength of the interference source. Clearly, the stronger the interference, the more deeply it is nulled. This property is typical of an entire class of nulling algorithms called *power inversion* algorithms.

Another property of nulling algorithms can be illustrated by assuming that the quiescent weight vector points an antenna beam at or near the location of the interference source; i.e., *b, c, d,* and *e* in Equation 5 are either zero or are very small. All the terms in $\mathbf{W}$ then are very small and the algorithm adapts to the interference by essentially shutting off the weights. This response is not always desirable because even a relatively small interferor can at least begin to shut the weights down and permit noise to dominate the received signal. To preclude this effect, many system designers find it advantageous to normalize the adapted weight; i.e.,

$$\mathbf{W}_{\text{optimum}} = \mathbf{W}\left(\mathbf{W}^{\text{H}}\mathbf{W}\right)^{-\frac{1}{2}}. \qquad (12)$$

The transient behavior of the nulling system is also of significant interest because many so-called smart jamming strategies have been proposed that attempt to defeat nulling systems by exploiting the transient response of the algorithm. The general form of the solution to Equation 4 is [2]

$$\mathbf{W}_{\text{transient}} = (\mathbf{v} - \mathbf{W})e^{-\frac{\alpha t}{\tau}} + \mathbf{W}, \qquad (13)$$

where $\mathbf{W}_{\text{transient}}$ is the transient value of the adapted weight, t is the time measured after the abrupt turn-on of an interferor, and α is proportional to the interference power. Similarly, the transient value of the adapted weight after the abrupt shutoff of the interferor is given by [2]

$$\mathbf{W}'_{\text{transient}} = (\mathbf{W} - \mathbf{v})e^{-\frac{t'}{\tau}} + \mathbf{v}. \qquad (14)$$

Equation 13 indicates that the adaption time of the

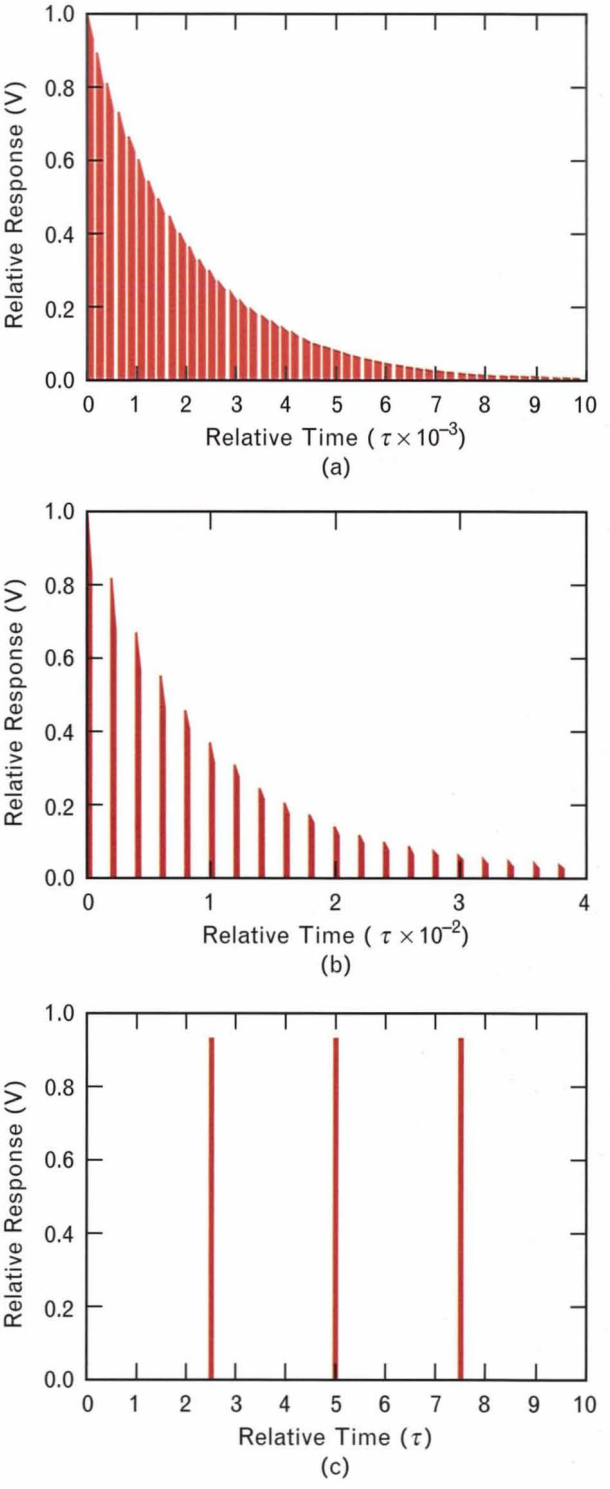

FIGURE 3. Response of nulling system to pulsed jamming. (a) The jammer is operating on 50% duty cycle with an on time equal to $10^{-4}\tau$, where τ is the circuit's RC time constant. (b) The duty cycle is reduced to 10% with an on time of $2 \times 10^{-4}\tau$. (c) The duty cycle is reduced further to 0.04% with an on time of $2 \times 10^{-3}\tau$.

system depends on the strength of the received interference signal; i.e., the system will adapt much more quickly to strong interference signals than it will to weak ones. Equation 14, however, indicates that if the interference is abruptly shut off the system will unadapt much more slowly than it adapted. Figure 3 illustrates the response of the system for three different interferor duty cycles. Note that an interferor with a very low duty cycle (Figure 3[c]) can have a periodic effect on the nulling system. Thus a communications system used in conjunction with the nulling system can, at worst, suffer periodic jamming by a pulsed jammer with a very low duty cycle (less than 1% for most nulling systems). Such interference, however, will have little or no effect on the performance of communications systems that use interleaving and coding to improve their robustness against interference as well as thermal noise.

Nulling-Antenna Considerations

Many military satellite communications systems use some form of spread-spectrum modulation on their communications signals. The modulation, which usually takes the form of pseudo-random sequence modulation or frequency hopping, is intended to force a jammer to spread its signal over a much broader bandwidth than would otherwise be necessary. Because the satellite receivers used are capable of despreading the communications signals without despreading the jamming signals, jammers must radiate considerable power to jam even weak communications signals effectively. Nevertheless, antijam spread-spectrum modulation by itself cannot often provide the desired link robustness; in such cases, adaptive antenna nulling is also required. Thus the ability to place a broadband null in the direction of a jammer is a desirable feature of a nulling system.

Also, military communications often involve message traffic to, from, and within an operating area that may be only a few hundred miles across, and many scenarios include jammers operating within one hundred miles or less of communications terminals. The nulling system must be capable of placing nulls on these jammers without also including the communicating terminals within the null. Because many military communications satellites orbit at geostationary altitude (22,300 mi above the surface of the earth), the nulling antenna aperture required to achieve the desired resolution must be many wavelengths in diameter. Consequently, two major and related issues in the design of antenna nulling systems for military satellite communications are those of nulling bandwidth and nulling resolution.

These two considerations—nulling bandwidth and nulling resolution—primarily dictate the choice of antenna type to be used in a satellite communications nulling system. Typically, two generic types of antennas are considered: the thinned phased array and the multiple-beam antenna.

The thinned phased array consists of a number of antenna elements distributed over a large aperture with the individual elements spaced many wavelengths apart, as opposed to more conventional arrays that use element spacings of less than one wavelength. One form of thinned phased array that has been studied in depth as a nulling antenna is the ring array [3], illustrated in Figure 4. For a given aperture size, the thinned phased array provides superior nulling resolution compared to alternative designs. But the thinned phased array suffers in its ability to produce broadband nulls and, because of its inherently high sidelobes, it must utilize nulling degrees of freedom to suppress jammers that are located well away

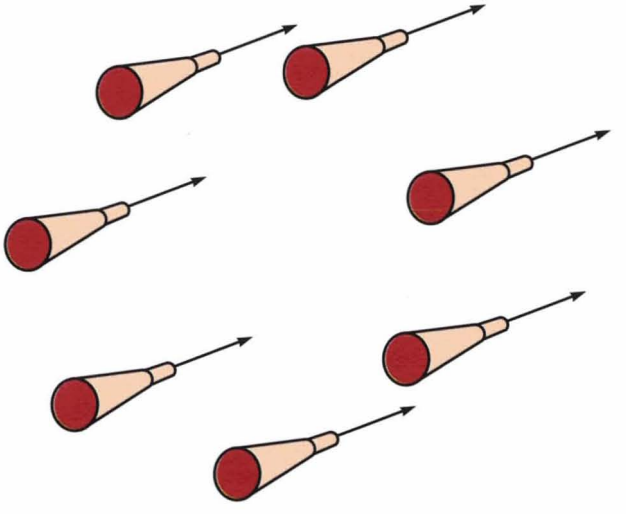

FIGURE 4. Seven-element ring array with horn antennas spaced equally around a circle. To suppress any interference, a seven-channel nulling circuit processes the signals received by each horn.

from the intended coverage area.

The multiple-beam antenna usually consists of a cluster of antenna feeds located in the focal plane of a collimating lens or reflector. The lens form of this antenna is illustrated in Figure 5. Each antenna feed produces a beam pointed in a specific direction, and the desired unjammed, or quiescent, antenna coverage is obtained by the suitable weighting and combining of the user signals received on each of the beams. For a given aperture size, the multiple-beam antenna has somewhat poorer resolution than the thinned phased array. But the multiple-beam antenna is capable of producing broadband nulls and, because it can be designed to possess low sidelobes, it does not require the use of nulling resources to suppress jamming signals that originate away from the intended coverage area.

The actual implementation of each of these antenna design concepts depends, of course, on the specific mission the antenna is expected to accomplish. In general, the thinned phased array is not particularly suitable for area coverage, although it is possible to construct one for such a purpose. The thinned phased array is much more useful as an antenna capable of providing one or more simultaneous beams that can, with electronic beam-steering techniques, be switched rapidly from user to user to provide agile beam service. In this application the antenna beam can be made as narrow as either beam-pointing uncertainties or satellite real-estate availability permits, thus maximizing the resolving power of the antenna. A thinned phased array designed to cover a limited area located anywhere on the visible earth would require each of the elements making up the array to have steerable (either mechanically or electronically) beams of a width commensurate with the angular size of the area as seen from the satellite.

The multiple-beam antenna, on the other hand, is well suited for area coverage because the size of the total beam cluster produced by the antenna can be made large enough to cover a given area. The resolving power of the antenna, however, depends on the size of the individual beams that make up the cluster; this size can be limited by satellite real-estate availability and complexity considerations. The multiple-beam antenna can be mechanically pointed to orient its beams on a given area or it can be constructed with enough beams so that, in the aggregate, they cover the entire visible earth, which subtends an angle of 17.3° at geosynchronous altitude. Generally, this latter design approach includes a switch network that connects a subset of antenna feeds to the nulling system for area coverage. With this configuration the multiple-beam antenna can also be used instead to provide one or more simultaneous beams for agile beam service.

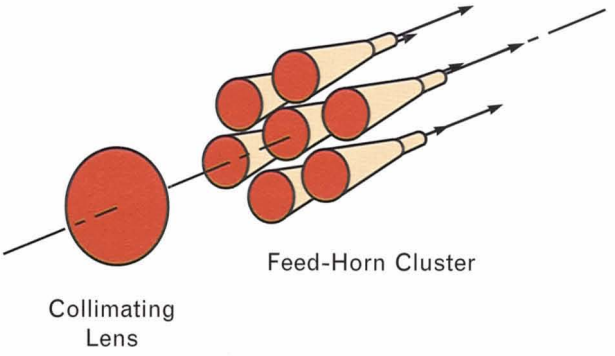

FIGURE 5. Seven-beam lens antenna with receive horns clustered in the focal plane of a collimating lens. Each horn produces a beam that points in a slightly different direction. To suppress any interference, a seven-channel nulling circuit processes the signals received by the horns.

Figure 6(a) shows the radiation pattern of one type of thinned phased array—a 150-wavelength-diameter ring array with seven equally spaced antenna elements designed to produce maximum antenna gain over the visible earth as seen from geosynchronous altitude. Note the high sidelobes and relatively narrow main beam, both characteristics of thinned phased arrays. In contrast, Figure 6(b) shows the radiation pattern of a single beam of a multiple-beam antenna with a 150-wavelength aperture. The beam is approximately 1.5 times broader at the half-power points than that of the thinned phased array, and the sidelobes are significantly lower. Figure 7 shows the radiation pattern of a 150-wavelength-diameter-aperture multiple-beam antenna with its seven beams weighted and combined to provide coverage over a 1°-diameter area (corresponding to an area 400 mi across).

Figures 8(a) and (b) illustrate the relative broadband-nulling capabilities of each type of antenna.

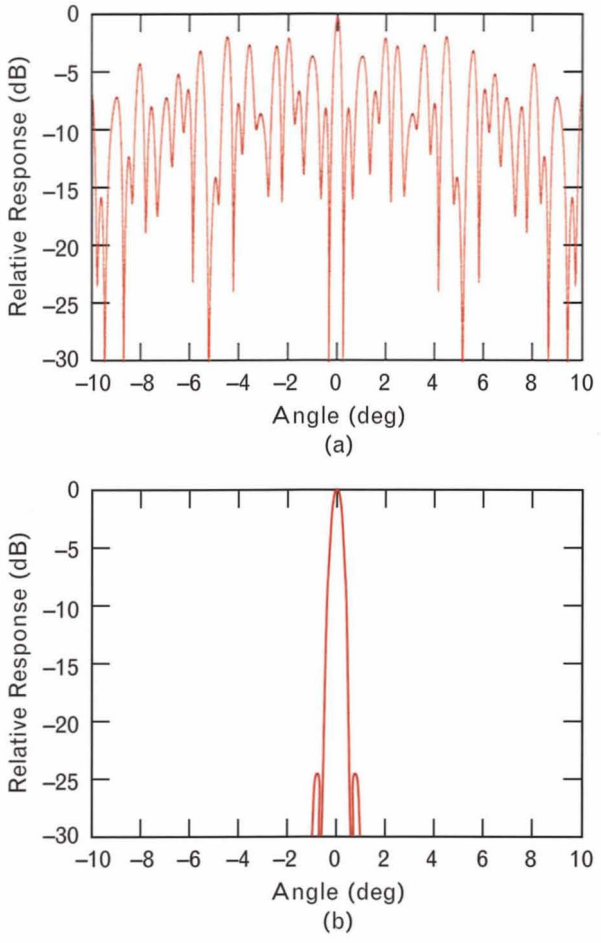

FIGURE 6. Antenna patterns for (a) seven-element ring array in which the horn antennas are arranged in a circle 150 wavelengths in diameter and each individual horn produces a pattern with a beamwidth equal to 15°, and (b) seven-beam lens antenna with an aperture diameter of 150 wavelengths and only one of the receive horns turned on.

The figures assume that there is no relative dispersion in the weighting and combining circuitry so that only the dispersive properties of the antennas act to limit the achievable null depths. On average, the null achievable with the multiple-beam antenna is about 15 dB deeper than that achievable with the thinned phased array.

Finally, Figures 9(a) and (b) illustrate the relative resolution of the two antennas. With the thinned phased array, a terminal attempting communications while located within 0.1° of a jammer will lose about 8 dB in gain due to nulling. With the multiple-beam antenna, a similarly located terminal would be well into the null and would probably be unable

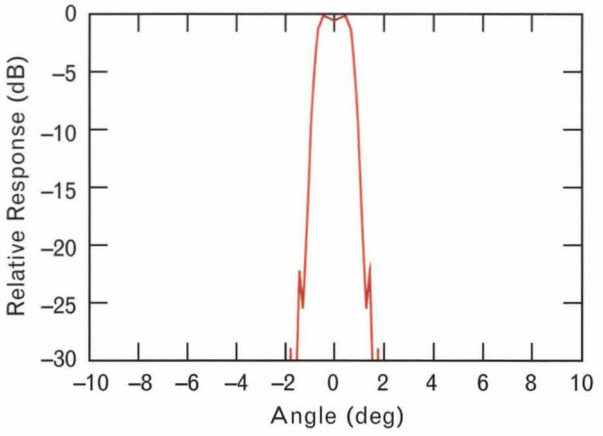

FIGURE 7. Composite pattern of seven-beam lens antenna with an aperture diameter of 150 wavelengths and all the receive horns turned on. The outputs of the horns have been summed into a single output.

to establish communications.

Various hybrid designs that involve a mixture of both types of antenna concepts have also been studied. In one of the more commonly considered concepts, each of the antenna elements in the thinned phased array is replaced with identical multiple-beam antennas. This concept permits the antenna designer to retain the high resolution inherent with the thinned phased array while reducing the sidelobe levels and dispersion of the antenna.

Figure 10 shows a block diagram of this hybrid concept using seven seven-beam antennas. The beam to a specific earth terminal is formed by using a switch network to select the appropriate beam from each of the seven-beam antennas. Lengths of transmission line placed between the seven-beam antenna feeds and the switch network introduce time delays that partially compensate for the dispersion of the array, thus improving the broadband nulling performance. Jammers located outside the selected beams of the seven-beam antennas are suppressed by the low sidelobes of the antennas rather than by nulling, thus allowing the system to concentrate its available nulling degrees of freedom on those jammers which are closer to the communicating terminal. Figure 11 shows a typical radiation pattern and the null depth over a 6% bandwidth for this type of antenna.

Although the above hybrid design does much to reduce the disadvantages of the thinned phased array as a nulling antenna, the ability to provide coverage

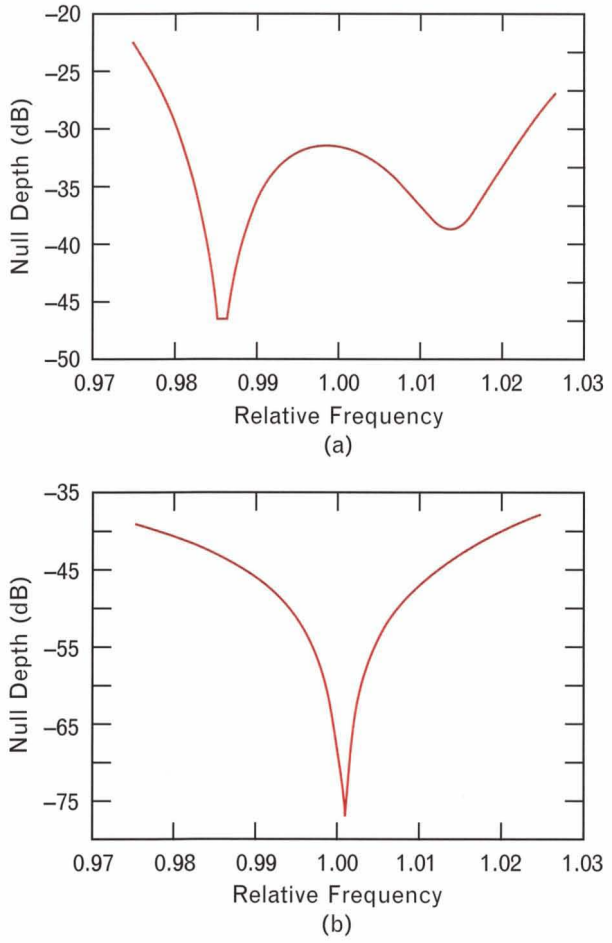

FIGURE 8. Null depth as a function of frequency for (a) seven-element ring array and (b) seven-beam lens antenna. In part *a*, a jammer is located in the sidelobes of the array pattern 6.4° away from the desired-signal direction (i.e., the pointing direction of the array beam). This large angular separation between the desired beam and the jammer results in poor nulling performance at the band edges due to antenna dispersion. In part *b*, a jammer is located 0.5° away from the desired-signal location within the antenna beam.

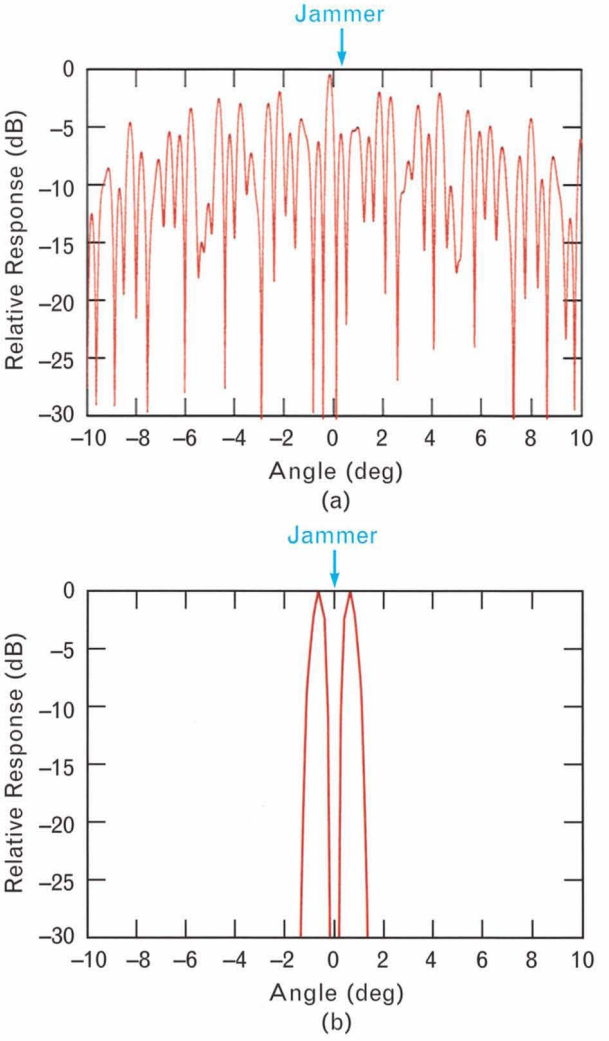

FIGURE 9. Adapted patterns showing the resolving power of the (a) seven-element ring array and (b) seven-beam lens antenna with all the receive horns turned on. In part *a*, a jammer is located at 0.1° and the desired signal at 0°. Note that the adaption process has cost the desired signal 8 dB in antenna gain. In part *b*, a jammer is located at the peak of the beam formed by the central horn. Note that a desired signal originating at a location within 0.1° of the jammer would be nulled along with the jammer.

over an area is still limited. In addition, the use of multiple-beam antennas as array elements rather than the relatively simple earth-coverage elements (previously described) radically increases the weight and complexity of the antenna. The antenna described in Figure 10 includes enough hardware to produce 49 beams and switch networks that select seven of the beams to provide inputs to a seven-channel nulling system. Including estimated antenna and switch-network losses, the antenna gain is about 31 dBi at the edge of the beam coverage area, and the *vulnerability* area (i.e., the area in which jammers are not suppressed by low sidelobes and must be nulled) is about 6° across, as shown in Figure 11(a). The vulnerability area is approximately one-third the width of the entire visible earth as seen from geosynchronous altitude. If system requirements dictate a higher antenna gain the designer could add more multiple-beam antennas to the array. A 3-dB increase in gain would

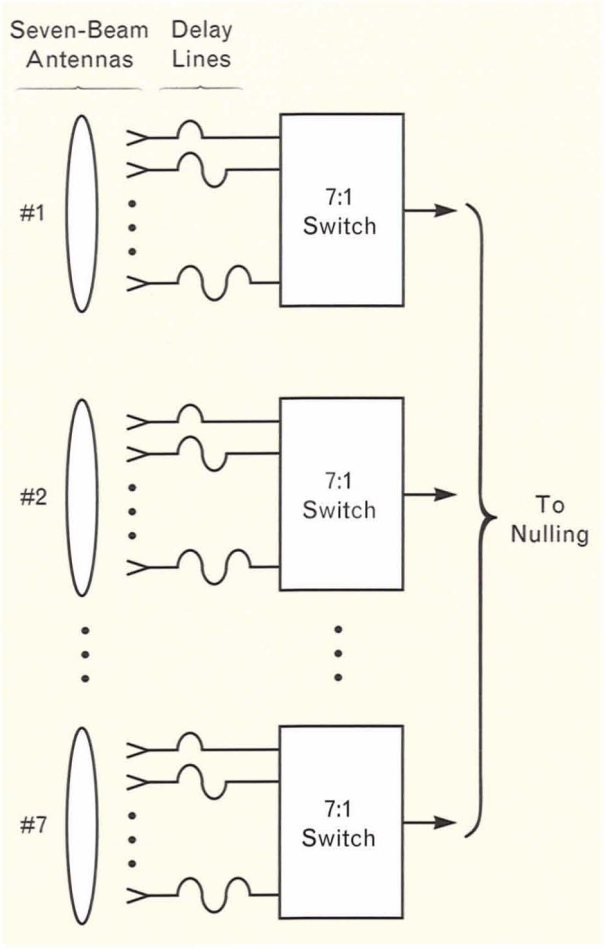

FIGURE 10. Hybrid design of thinned phased array with seven seven-beam antennas. The figure illustrates how seven of the lens antennas shown in Figure 5 might be used in a thinned-phased-array configuration. Switch networks are used to select one of the relatively narrow beams from each lens antenna. Each of the seven beams in an antenna element points in the same direction so that one antenna element can illuminate only a portion of the earth. The capability to switch from one antenna element to another enables the overall antenna system to cover the entire visible earth.

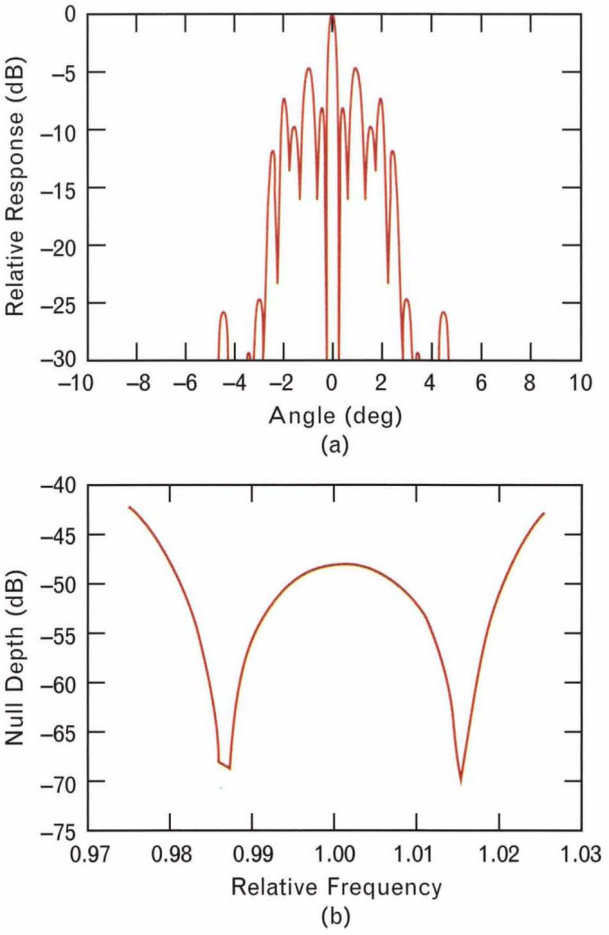

FIGURE 11. Antenna characteristics of the hybrid system shown in Figure 10: (a) radiation pattern and (b) null depth. Although the sidelobes in the radiation pattern are still high, they fall off much more quickly than those shown in Figure 6(a). Thus it would not be necessary to use nulling resources to suppress jammers located well away from the area of interest. In part *b*, a jammer is located 2.7° away from the desired-signal direction. (Note that the location is closer than that of the jammer in Figure 8[a]). Because of the reduced antenna dispersion, the null is significantly deeper than that shown in Figure 8(a).

require the addition of at least seven more seven-beam antennas to the system, increasing the number of beams to 98 and the number of nulling channels to 14, but leaving the width of the vulnerability area at 6°. Alternatively, the use of seven 19-beam antennas would achieve an increase in gain of about 4 dB without the need to increase the number of nulling channels. This design reduces the width of the vulnerability area to about 4° but increases the number of beams to 133. This antenna concept, however, still suffers from an inability to provide effective area coverage.

The multiple-beam antenna, on the other hand, can provide excellent area coverage and, if equipped with enough beams to cover the visible earth, can also be used to switch beams rapidly from one user location to another for agile beam service. But this design also has its limitations. A 150-wavelength-diameter multiple-beam antenna produces individual beams

with a half-power width of about 0.6°. Thus 721 beams would be required to cover the visible earth. Clearly, complexity and weight are significant issues when this type of antenna design is considered for satellite communications. One of the major complexity issues is that of the switch network, which must connect a subset of the 721 antenna feeds to the nulling circuits.

A switch network that could connect, for example, seven arbitrarily selected beam feeds out of a total of 721 to the nulling circuits would require thousands of single-pole double-throw (SPDT) radio frequency (RF) switches. A network that selects an arbitrarily located cluster of seven beams, however, is somewhat simpler, requiring 714 switches. The switching algorithm is illustrated in Figure 12. All of the family of antenna feeds labeled 1 are connected to a single binary switch tree that selects one of these feeds. Similarly, the families of feeds labeled 2, 3, 4, 5, 6, and 7 are also connected to binary switch trees so that it is possible to connect one member of each family of feeds to the nulling circuitry. Appropriate selections from each family can then result in any arbitrarily located hexagonal cluster of feeds being connected to the nulling circuitry. For area coverage, all of the beams in the cluster are turned on to form a beam similar to that shown in Figure 7. For agile beam service, the cluster most nearly centered on the communicating terminal is selected, and the nulling system weights the selected cluster's central beam on and the peripheral beams off.

Although multiple-beam antennas incorporating hundreds of beams have been studied both at Lincoln Laboratory and elsewhere [4], none have progressed beyond simple feasibility demonstrations. The antennas studied represent a significant investment in weight and complexity and are capable of providing either area coverage or agile beam service as required but incapable of providing both simultaneously. Many requirements for satellite communications, however, call for simultaneous area coverage and one or more electronically agile beams. Providing such service with this concept for a multiple-beam antenna requires an antenna for each independent beam, thus compounding the investment in satellite weight.

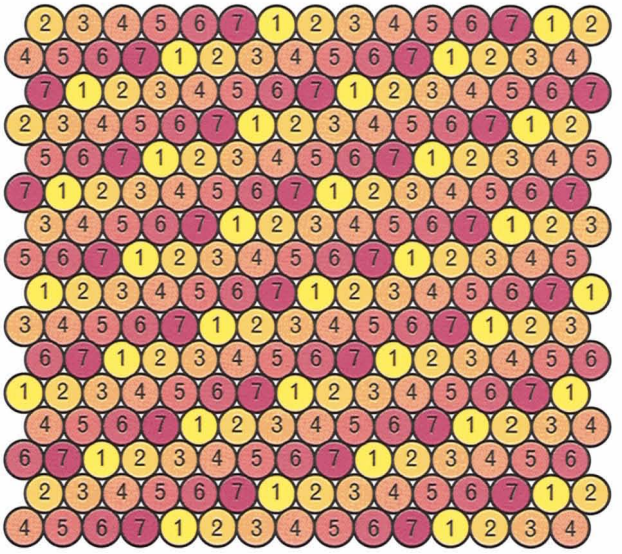

FIGURE 12. Select Seven switch-connection algorithm. The figure shows a cluster of receiving horns, as might be arranged on a triangular grid lying in the focal plane of a lens antenna similar to that shown in Figure 5, but with many more beams. The output of each horn is connected to a binary select-one-of-many switch tree. Those horns labeled with a 1 are connected to switch tree 1, those labeled 2 are connected to switch tree 2, and so on. It is possible, then, to select *any* hexagonal cluster of seven beams by selecting the appropriate horn from each of the seven switch trees.

A Recent Nulling-Antenna Development

Lincoln Laboratory has been investigating a different multiple-beam antenna concept that combines the high-resolution features of the thinned phased array with the area-coverage and agile-beam capabilities of the multiple-beam antenna. This 56"-diameter antenna [5], illustrated in Figure 13, is designed to operate in the 43.5-to-45.5-GHz satellite communications band and is capable of simultaneously providing area coverage and two independently agile beams. The antenna consists of seven multiple-beam antennas arranged in a hexagonal cluster. The central antenna produces 19 beams while the peripheral antennas produce 18 beams each for a total of 127 beams.

One fundamental difference between this antenna and the thinned phased array of multiple-beam antennas described earlier is that the beams from this antenna all point in different directions. The half-power beamwidths, however, are such that adjacent

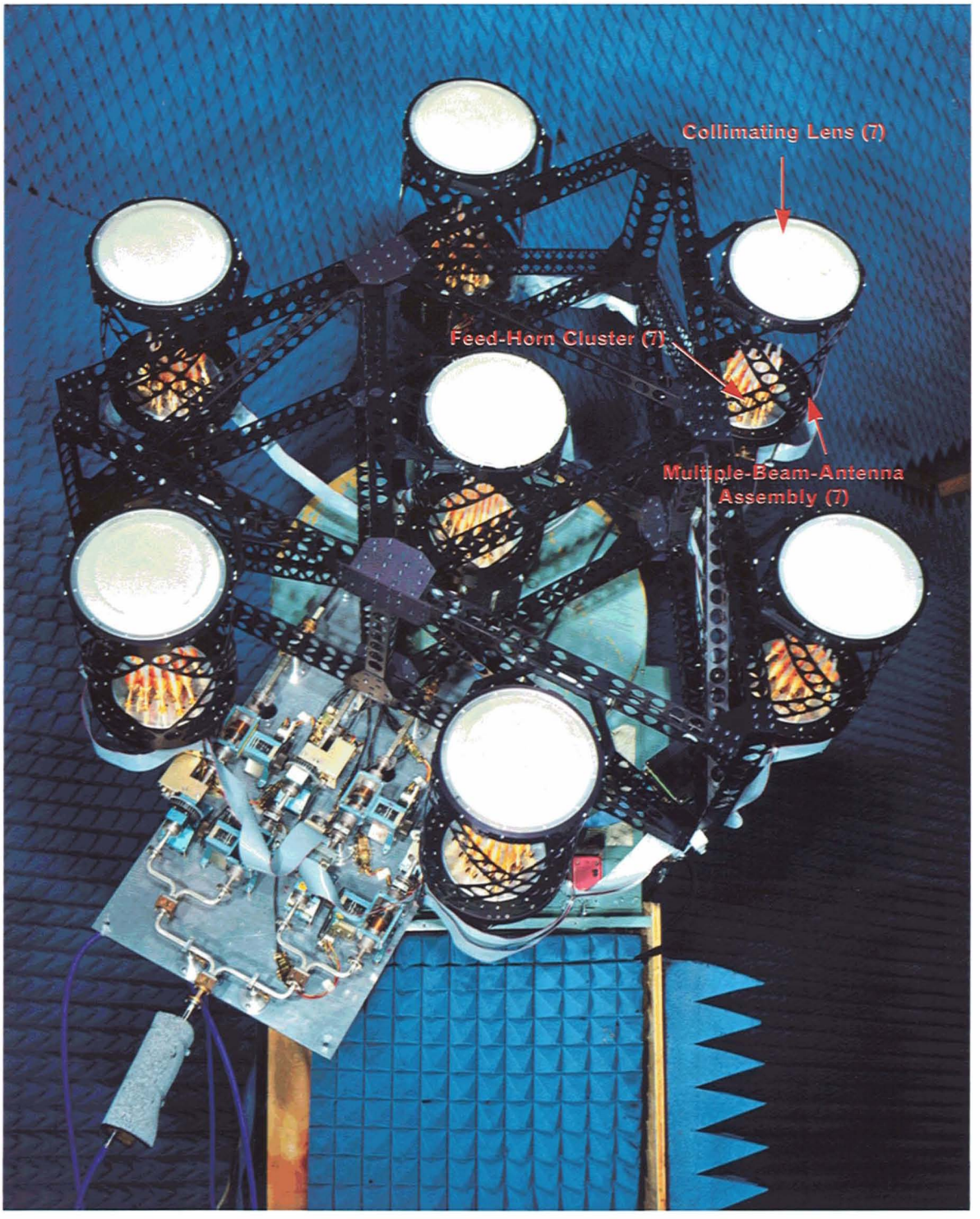

FIGURE 13. Seven-lens multiple-beam antenna, recently developed at Lincoln Laboratory. The antenna design combines the high resolving power of the thinned phased array with the low dispersiveness and sidelobes of the multiple-beam lens antenna for superior nulling performance. Weighing only 56 lb, the antenna operates in the 44-GHz satellite communications band to provide three independent and electronically agile beams for simultaneous service to a 1.5° area and individual users located anywhere within a satellite field of view. A brassboard four-channel nulling circuit is shown in the lower left portion of the photograph.

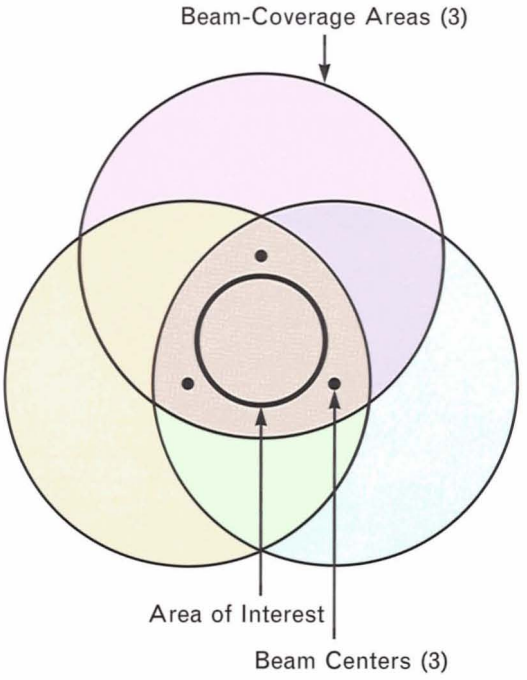

FIGURE 14. Beam overlap of three adjacent beams, each selectable with a different switch tree, as in Figure 12. Regardless of its location, the center of an area of interest will always lie on the edge or within a triangle formed by three beam centers. Thus the center of any arbitrarily located area up to 1.5° (600 mi) across will always lie within, and can therefore be serviced by, a single beam. Similarly, any single communicating terminal will also lie on the edge or within such a triangle. (Note, however, that the triangle does not have to be the same triangle that contains the center of the area of interest.) Although the selection of a single beam (and, hence, the selection of a single switch tree) for area coverage prevents the selection of any of the other beams connected to the same switch tree, two other beams from two other switch trees can be used to provide service to two arbitrarily located terminals.

beams overlap to a considerable extent, as illustrated in Figure 14. The effect of this overlap is that any arbitrarily located area up to 1.5° (600 mi) across will always lie completely within a single beam and any location on the surface of the earth will always lie within at least three beams. With a suitable switch network, then, it is possible to provide both coverage to a 1.5°-wide area and simultaneous dual independent agile beam service simply by the appropriate selection of three beams.

In practice, the antenna developed is configured for the selection of 14 beams, three to provide service

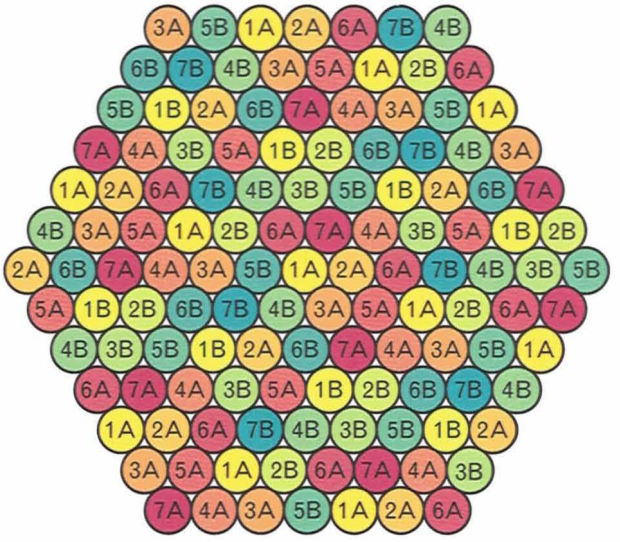

FIGURE 15. Feed-to-switch-tree connections for seven-lens antenna. The figure illustrates the switching algorithm used to select beams. There are 14 switch trees, two per lens assembly, to produce 14 outputs. The numbering system identifies the lens assembly and the switch tree associated with that lens. For example, 5B denotes the B tree in lens assembly 5. Note that any three-beam cluster is made up of beams from different lens assemblies.

in an unjammed environment and 11 to provide the degrees of freedom for nulling. Figure 15 illustrates the switching algorithm used to connect the antenna beam feeds to the nulling circuitry. Two beams are selected from each of the seven multiple-beam elements. Thus the family of beam feeds labeled 1A are those feeds selectable by switch tree A of multiple beam antenna 1.

Although it may initially appear to be haphazard, the switching algorithm shown in Figure 15 does contain features that help simplify the fabrication and assembly of each multiple-beam antenna. Figure 16 illustrates this fact. In Figure 16(a), the relative locations of the lens feeds for antenna 1 are shown. The locations are arranged in a 19-feed hexagonal array and connections to the switch trees are such that a single-pole four-throw (SP4T) switch could be used as the basic building block for the switch network. Figures 16(b) and (c) show the feed arrangements for antennas 2 and 6, respectively. These figures also suggest the use of SP4T switches, but, more importantly, the two arrangements are identical; one is simply

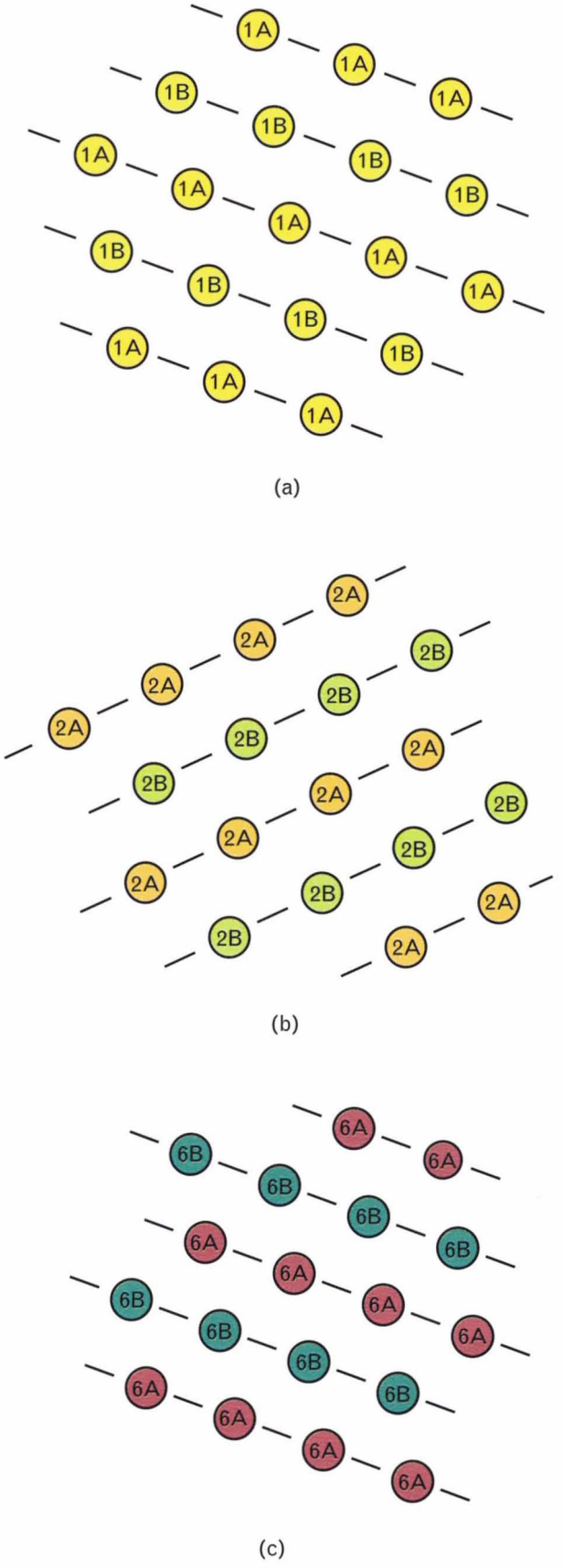

rotated relative to the other. In fact, the feed arrangements for antennas 2 through 7 are all identical except for their relative angular orientations. Thus the antenna system consists of a central, relatively simple, 19-beam antenna surrounded by six equally spaced identical 18-beam antennas.

Description of Hardware

The RF switch structure and the switch drive electronics were manufactured for Lincoln Laboratory by Electromagnetic Sciences, Inc. (EMS) [6], of Norcross, Ga. An SP4T switch structure was used for the basic switching element (Figure 17). The structure consists of seven SPDT ferrite circulator switches integrated into a monolithic waveguide structure. Four of the switches are used as isolator switches to ensure that those feeds which are switched off are isolated from the switching circuit output by at least 40 dB. The ferrite circulator switches have excellent RF properties: insertion loss of ~0.1 dB, isolation greater than 20 dB, and switching time less than 1 μsec. Figure 18 shows a sketch of the complete waveguide switch structure for one of the 18-beam antennas.

The switch drive electronics accept transistor-transistor logic (TTL) commands specifying the appropriate switch trees and feeds to be selected. After determining which switches require switching, the drive electronics perform the operation in less than 1 μsec. The drive electronics are mounted on the lightweight frame that encloses the switch structure for each antenna element (Figure 19). When reconfiguring the antennas to select different groups of 14 beams at a rate of 10,000 reconfigurations/sec, the switching circuits draw a maximum power of about 9 W.

The antenna feed horns were developed at Lincoln

FIGURE 16. Feed-to-switch-tree connections for (a) lens feed 1, (b) lens feed 2, and (c) lens feed 6. The figures illustrate the feed-cluster layouts for the lens assemblies. Part *a* shows the layout for the central assembly. The alignment of feeds connected to the A and B switch trees has been chosen such that interlacing of the tree structure is minimized. Parts *b* and *c* show the layouts for two other assemblies. Note that the layouts are identical; one is simply rotated relative to the other. In fact, the outer six assemblies (numbers 2 through 7) are identical except for their relative angular orientations.

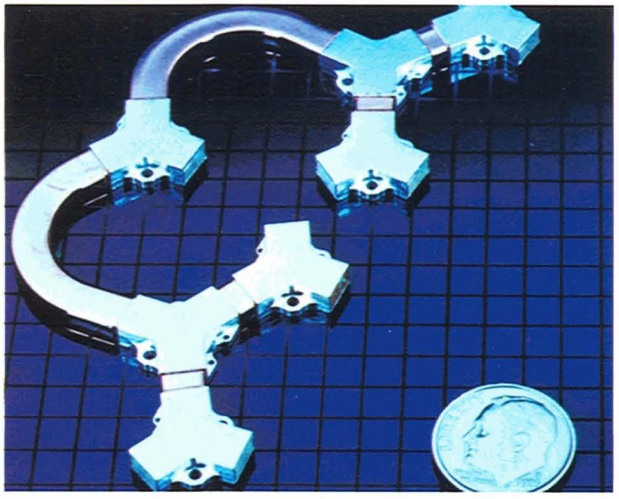

FIGURE 17. Single-pole four-throw (SP4T) monolithic RF switch structure, the basic building block of all the switch trees in the antenna. Manufactured by Electromagnetic Sciences, Inc., of Norcross, Ga., the switch structure consists of seven single-pole double-throw (SPDT) ferrite circulator switches integrated into a monolithic waveguide structure. The total weight is less than 0.6 oz, a factor of 10 lighter than similar switch structures manufactured with conventional flanged waveguide technology.

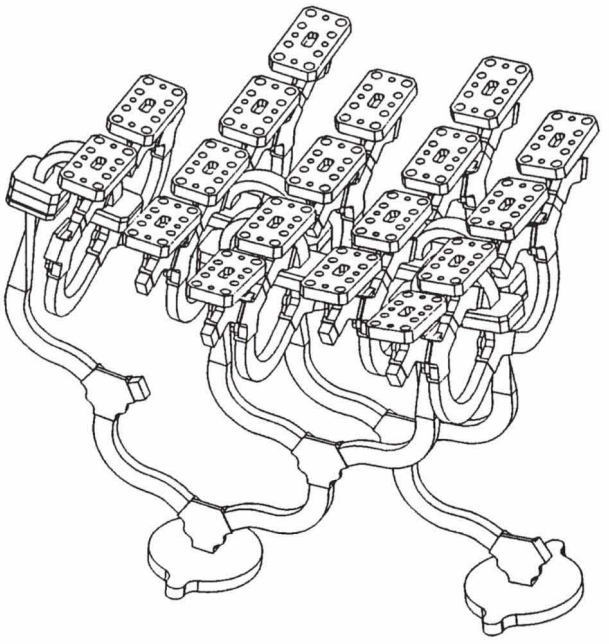

FIGURE 18. Complete switch-tree structure for an outer lens assembly (numbers 2 through 7) with 18 inputs and two outputs.

Laboratory; every effort was made to arrive at a design that would result in an extremely lightweight but rugged feed horn with good electrical performance. Several alternative designs were investigated in detail before the final design was adopted. The feed horns developed for use in the antenna are made of thin-walled electroformed copper (Figure 20). Each horn contains a dielectric-vane polarizer to form the desired right-hand circularly polarized beams, a small resistive card to absorb any left-hand circularly polarized signals, and a thin dielectric tube protruding from the horn aperture to reduce the radiation-pattern beamwidth of the horn and improve the efficiency of the antenna. Each feed horn weighs 0.27 oz. Because the feed is long and thin and is structurally attached to the antenna only at one end, the horn was subjected to military-specification vibrations to ensure that it could withstand a launch environment. The feed horn survived the tests with no difficulty.

The 8"-diameter collimating lens that forms the antenna beams is made of a low-loss dielectric material. The lens surfaces, both front and rear, have been machine grooved to minimize signal reflections. In addition, the rear surface of the lens is zoned to minimize its weight. The collimating lens weighs 1.2 lb; it is the heaviest single part used in the antenna.

A thin aluminum plate serves as the mounting base for the switch structure, its support frame, and the switch drive electronics, as well as for the feed horns (Figure 19). The feed horns are connected directly to the switch output ports through rectangular openings machined in the plate.

The feed-horn/switch-structure assembly is attached to one end of a lightweight cylindrical aluminum structure and the collimating lens is attached to the other end to form the complete multiple-beam-antenna assembly. Captivating spring clips are used to secure the lens to the lens holder. The clips allow the dielectric lens to expand thermally relative to the aluminum lens holder without the buildup of stresses that could distort the structure or even crack the lens. The antenna developed by Lincoln Laboratory uses seven multiple-beam-antenna assemblies (Figure 13). Each assembly weighs 6.1 lb.

One of the major design goals of the multiple-beam-antenna assembly was to minimize weight without sacrificing the stiffness and strength necessary for the antenna to survive the rigors of a rocket launch.

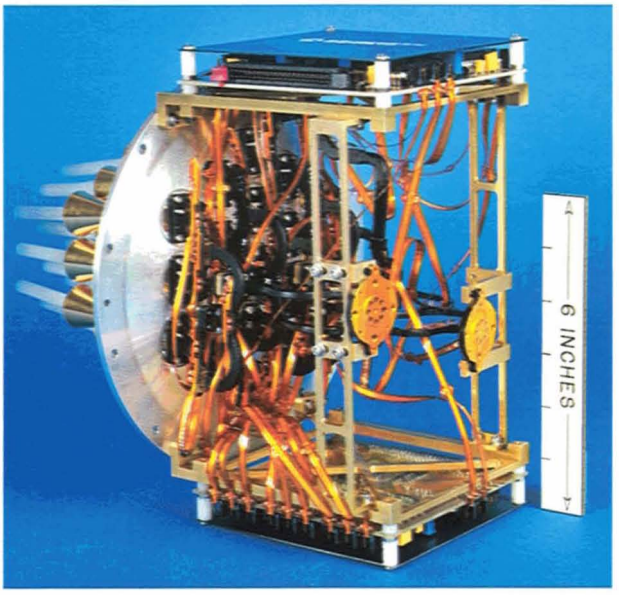

FIGURE 19. The complete switch and switch-drive assembly. The mounting plate for the lens and lens-holder assembly and the feed horns can be seen in the left rear. The feed horns are connected directly to the switch output ports through rectanglar openings machined in the thin aluminum mounting plate. The switch drive electronics, mounted on the top and bottom of the switch-assembly support cage, accept transistor-transistor logic (TTL) commands specifying the appropriate switch trees and feeds to be selected. Ribbon cables are used to connect the switch drivers to the switches. The entire structure weighs slightly more than 2 lb.

Accomplishing this goal required the development of original design approaches by EMS and Lincoln Laboratory engineers.

It was clear that fabricating the switch trees as monolithic thin-wall structures rather than as the more conventional flanged waveguide assemblies would result in major weight savings. Because a significant portion of the switch trees behind every lens could be fabricated with identical SP4T switch assemblies, it was decided for cost reasons that these trees would be built as integral structures. A second set of nearly identical flangeless switch assemblies would be used to interconnect the SP4T units to complete the switch trees. Flanges would be used to make the interconnections.

As described earlier, the SP4T units incorporated seven ferrite circulator switches (including four isolator switches). The switches, housed in lightweight nickel-silver-plated aluminum bodies, were interconnected by using thin-walled electroformed copper waveguides. A low-temperature solder connected the switch bodies and waveguides to form the complete assembly. EMS engineers developed an automated jigging fixture that was used during the assembly and soldering process to ensure that each of the switch assemblies was dimensionally identical within the extremely close tolerances required. The resulting SP4T switch assemblies have excellent electrical performance and weigh 0.55 oz each. Comparable SP4T switch assemblies fabricated with conventional flanged technology weigh 5.6 oz, more than 10 times as much.

Similar reductions, not only in weight but in power as well, were made in the switch drive electronics. Recent technology advances in thick-film complementary metal-oxide semiconductor (CMOS) integrated circuits and an innovative design approach resulted in a reduction (relative to previously manufactured drivers performing similar functions) of a factor of 4 in parts count, a factor of 3 in circuit board area and weight, and a factor of 1½ in power.

These efforts have resulted in seven switch-tree assemblies with a total of 127 inputs and 14 outputs designed to survive both the launch and orbit environments. The assemblies have a total weight of less

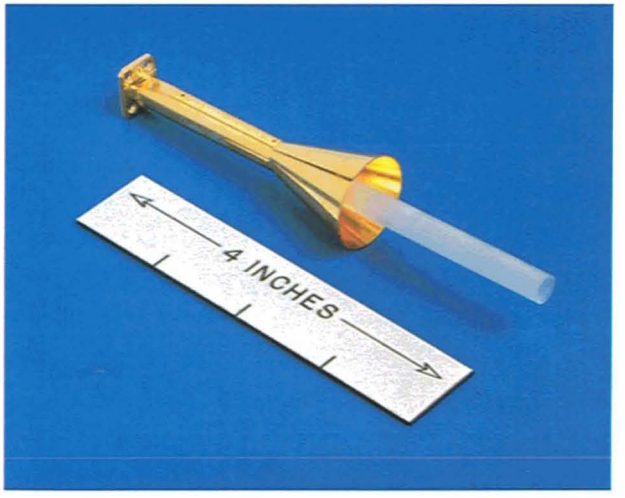

FIGURE 20. One of the 127 lightweight circularly polarized feed horns used in the antenna. The long tube protruding from the flared end of the horn makes the beamwidth of the horn more narrow than it would otherwise be, thereby increasing the overall efficiency of the antenna. Each horn weighs 0.27 oz and operates at 44 GHz.

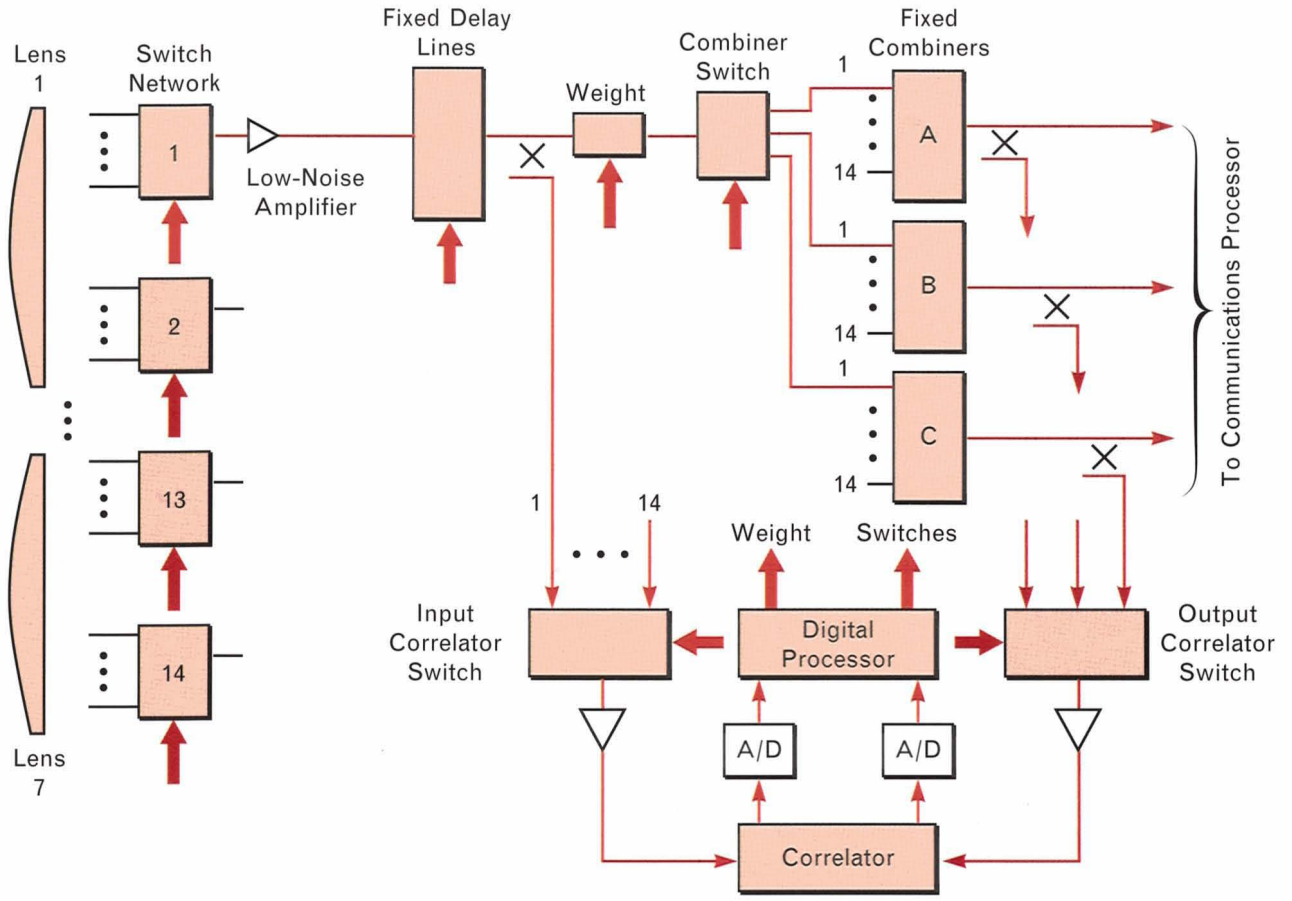

FIGURE 21. Nulling-processor architecture. Two switch trees behind each lens select 14 beams for input to the nulling processor. Three of the beams are service beams; the remaining 11 provide nulling degrees of freedom. Because desired signals can originate from widely different locations in a field of view, the 11 channels can be selected to correspond to a few beams clustered around each of the three beams chosen to service three signal sources. When this selection is made, the combiner switch selects the appropriate nulling channels to be applied to each of the three combiners. The combiners' outputs are applied to the inputs of three receivers, each processing a different desired signal. Fixed delay lines compensate for antenna dispersion while low-noise amplifiers provide signal preamplification on each channel to counter the effects of losses in the nulling circuit. The nulling algorithm is implemented in a digital rather than analog fashion: the correlator outputs are digitized with the filtering, amplification, and subtraction from the desired weight vector performed digitally. This approach maximizes the thermal stability of the circuit.

than 15 lb, which includes the mechanical support structure. In contrast, switch-tree assemblies with 38 inputs and a single output manufactured by EMS using more conventional design approaches weigh 20 lb.

Lincoln Laboratory's mechanical engineers designed and fabricated a very lightweight triangular aluminum structure to serve as a mount for the seven multiple-beam-antenna assemblies. The structure (as well as the antenna assemblies) was designed to withstand the shock and vibration environment experienced during the launch of a satellite by an unmanned rocket. The structure weighs 13 lb; the entire fully assembled antenna weighs only 55.8 lb. This weight is significantly less than that achievable with more conventional technology and it is low enough to make this antenna (or one of a similar design) a viable candidate for satellite communications.

Description of Nulling Algorithm

Figure 21 shows a block diagram of the nulling circuit envisioned for use with the antenna described above. The switch trees connect 14 beam feeds to the nulling circuit. Three of the beams are service beams; the

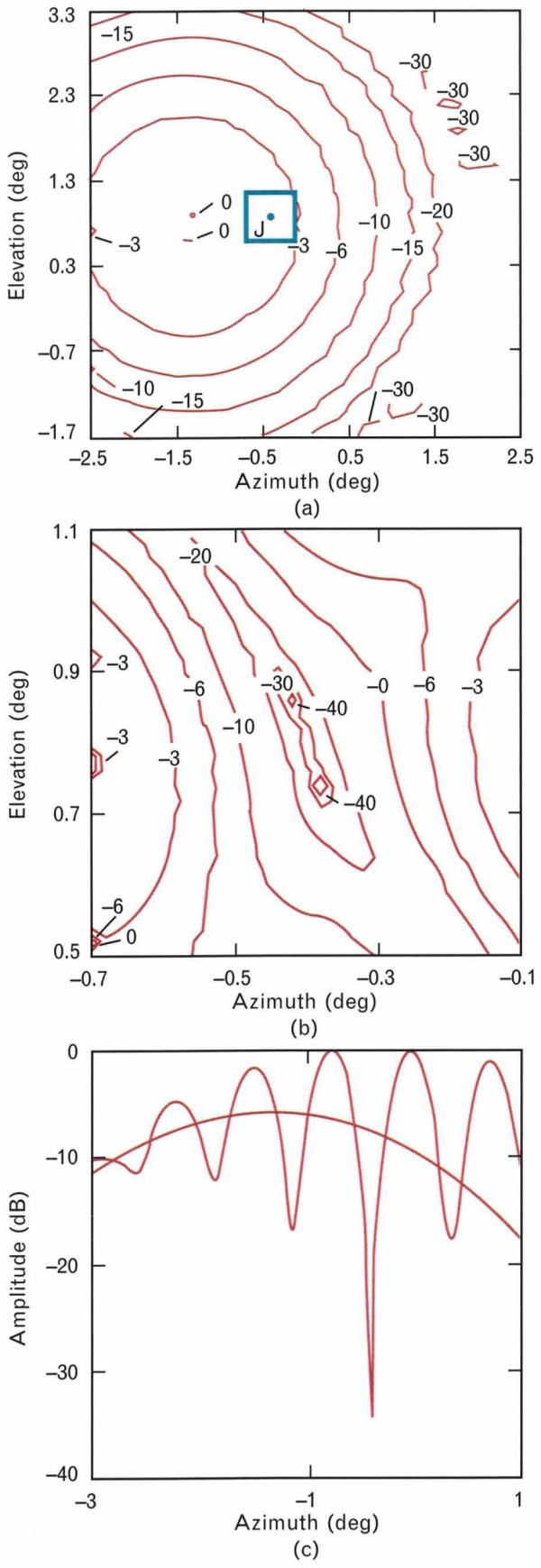

remaining 11 provide nulling degrees of freedom. Thus three clusters of beams are available for selection, each cluster consisting of a service beam and several surrounding beams. Either a prioritization algorithm or a direct command from a control center determines which of the surrounding beams is associated with each service beam. Based on which beams are selected, the on-board controller determines the time delays to switch into the circuit to minimize antenna dispersion. The controller also connects each channel to the appropriate combining circuit.

The nulling algorithm used is the modified Howells-Applebaum algorithm described earlier. In the algorithm a shared correlator provides sequentially sampled I and Q correlations of the appropriate output signals with the weight input signals. The nulling processor digitizes these correlations and computes the weights to be applied to the nulling channels. Nulling a jammer requires several correlation cycles. One of the many possible computations the processor could use to compute the weights is a modified form of Equation 1 called the steepest-descent algorithm [2]:

FIGURE 22. Nulling performance with single jammer: (a) Contour plot (in dB) of the measured radiation pattern of a single beam prior to adaption. The area of interest lies within the –3-dB contour between 0° and –2.5° azimuth and 0° and 1.9° elevation. A jammer is shown located at –0.4° azimuth and 0.85° elevation. (b) Measured pattern after adaption. The plot covers the area within the box shown in part *a*. Note the high nulling resolution attainable with the antenna: the angular difference between the null location and the –10-dB contour in azimuth is on the order of 0.1°. The poorer resolution obtained in elevation is due to the limitations of the four-channel nulling circuit used for the test. The circuit was connected such that the full antenna aperture was used in azimuth but only half the aperture was used in elevation. (c) Measured radiation pattern cuts taken in azimuth at the elevation location of the jammer. The smooth curve is the radiation pattern taken before adaption and the rippled curve is the result after adaption. Note the depth of the null achieved. The adapted pattern also shows some loss in gain to terminals that might be located 0.5° or more away from the jammer. Such gain losses are tolerable because terminals operate with an excess signaling margin of 10 dB or more to compensate for weather effects.

$$\mathbf{W}_n = \mathbf{W}_{n-1} + k\left(\mathbf{v} - \mathbf{B}_n\right),$$

where $\mathbf{W}_n$ is the set of weights to be installed on the nth cycle, k is a constant that controls the rate at which the nulling loop converges to a steady state, and $\mathbf{B}_n$ is the set of correlation samples measured on the nth cycle.

Test Results

Because the nulling circuit shown in Figure 21 has not yet been implemented, the antenna performance was tested with a simple four-channel nulling circuit that utilized stepper-motor-driven attenuators and phase shifters as weights. The lower left portion of Figure 13 shows this setup with the antenna mounted on a test stand in Lincoln Laboratory's anechoic test chamber. In the nulling-performance tests, one or two jammer sources were placed at appropriate locations within the antenna field of view, the beam responses to these sources were measured at several frequencies within the 43.5-to-45.5-GHz band, and the adapted weights were computed in accordance with Equations 2 and 12. The computation was performed by a personal computer. After determining the weights, the computer controlled the stepper-motor drives in the nulling circuit to set the weights; radiation patterns of the adapted array were then measured.

Figure 22 displays some of the results of the tests in which a single jammer was used. Figure 22(a) is a plot of the relative gain contours of the antenna with a single beam turned on to cover an area centered on –1.45° azimuth and 0.8° elevation. A jammer is shown located within the beam coverage area (i.e., within the –3-dB contour). Figure 22(b) shows the gain con-

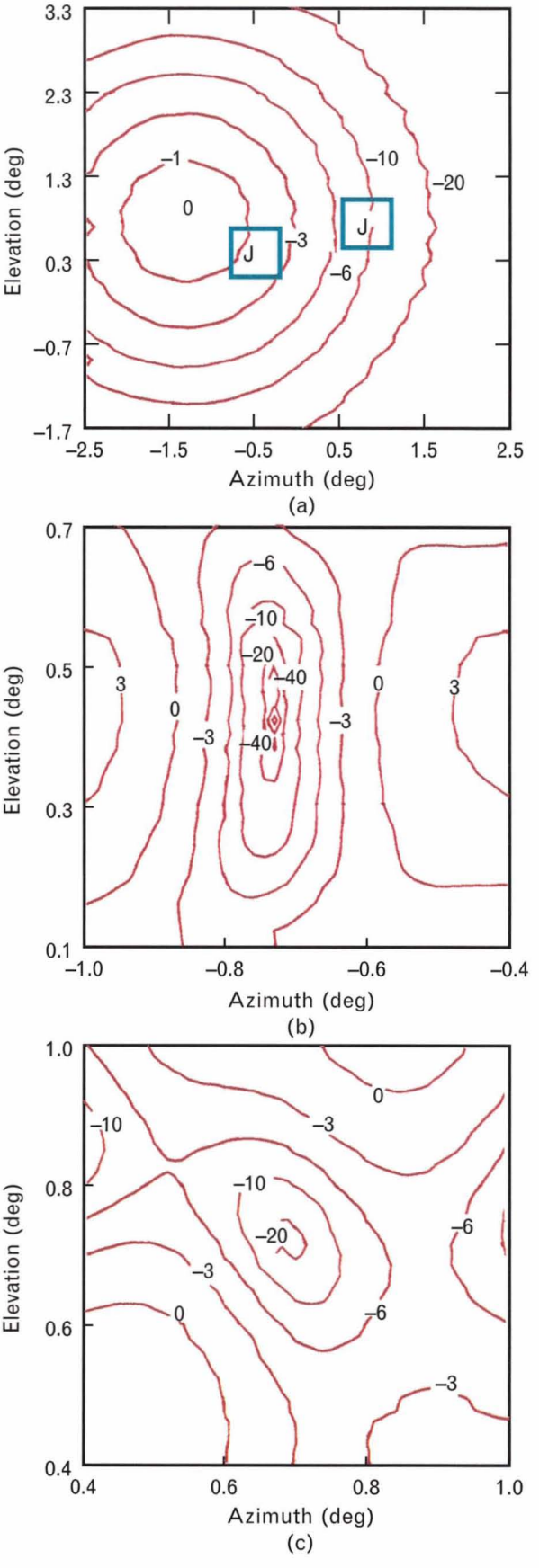

FIGURE 23. Nulling performance with two jammers: (a) Measured contours (in dB) of an area-coverage beam prior to adaption, as in Figure 22(a). In this case, however, two jammers are present: one at –0.7° azimuth and 0.4° elevation, and the other at 0.7° azimuth and 0.7° elevation. (b) Measured adapted contours for jammer located at –0.7° azimuth and 0.4° elevation. (c) Measured adapted contours for jammer located at 0.7° azimuth and 0.7° elevation. Note the ability of the antenna to maintain high-resolution nulling while dealing with a multiple-jammer attack.

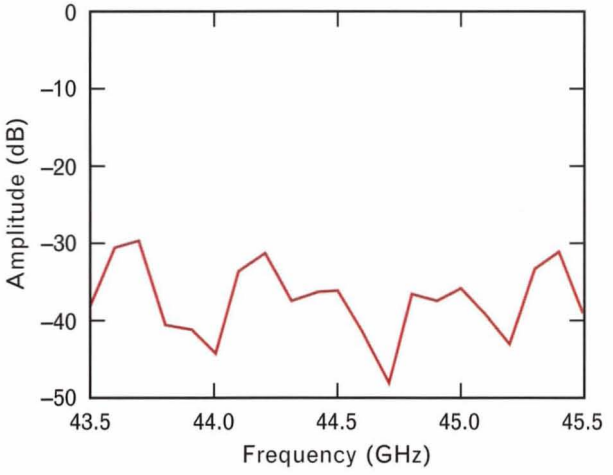

FIGURE 24. Null depth versus frequency for the adapted null shown in Figure 22. Note that the antenna is capable of achieving a broadband null with a depth of at least 30 dB over the frequency band from 43.5 to 45.5 GHz.

tours (measured relative to the peak gain shown in Figure 22[a]) of the adapted radiation pattern. The area shown is that defined by the box in Figure 22(a). Figure 22(b) illustrates the sharpness of the null: the –10-dB-or-higher contours are less than 0.1° in azimuth away from the 30-to-40-dB null. Figure 22(c) shows the measured azimuth radiation pattern of the adapted antenna. Note that the null in the figure is about 35 dB deep. The ripples are characteristic of the thinned phased array, but they do not have minima as deep as those shown in Figure 11(a) because the beams from the individual multiple-beam antenna elements do not fully overlap in this design. Consequently, the ripples in the pattern are not deep enough to disrupt communications.

Figure 23 displays measured results taken in a two-jammer scenario. Figure 23(a) is a plot of the quiescent coverage with two jammer locations identified, one inside the coverage area and one just outside. Figures 23(b) and (c) show the measured adapted patterns, again of the areas within the boxes around the jammers. The figures illustrate the high resolution of the antenna.

Figure 24 shows the frequency behavior of the null of Figures 22(b) and (c). In the figure the relative dispersion of the antenna, the switch-tree structure, and the nulling circuitry have been well controlled, and a broadband null with a depth of at least 30 dB has been achieved within the 43.5-to-45.5-GHz band.

Summary

This article familiarizes the reader with some of the more important considerations involved in the design of adaptive nulling antenna systems for military satellite communications. The basic nulling-circuit configuration is briefly presented and some of the mathematics describing the performance of a particular circuit, the modified Howells-Applebaum circuit, is considered.

Discussions regarding the various options available to the nulling antenna designer conclude that, although the thinned phased array has excellent nulling resolution, it is not a good candidate for area coverage. The multiple-beam antenna, on the other hand, can provide good area coverage but has poorer nulling resolution. The thinned phased array and multiple-beam antenna can both be constructed for electronically agile beam service.

Because of the disadvantages of both types of antennas, Lincoln Laboratory has constructed and demonstrated an antenna system that combines the desirable qualities of both antennas with the added advantages of multiple simultaneous beam service and extremely light weight. The 43.5-to-45.5-GHz antenna, designed to withstand the rigors of both a launch and a space environment, produces three simultaneous electronically agile beams, any one of which can be used for area coverage. The antenna can achieve broadband nulls at least 30 dB deep with a resolution of about 0.1°. Weighing slightly less than 56 lb, the antenna is a viable candidate for military satellite communications.

Acknowledgments

Much of the discussion in this article is derived from the work of many people at Lincoln Laboratory and elsewhere. Because of the number of people involved, the author cannot include in this paragraph every person whose work deserves acknowledgment. For this, the author ruefully apologizes. People whose names come to mind, however, are Dr. Bing Potts, who directed the development of the seven-lens antenna from its inception to near completion; Drs. Lawrence Rispin and Alan Fenn, who completed the job; Frank Folino, who was responsible for the me-

chanical design; Kurt Zimmerman of Electromagnetic Sciences, Inc., who directed the development of the RF switch trees; Dr. Andre Dion, who designed the collimating-lens structure of the multiple-beam antenna elements; Dr. Joseph Lee, who designed and developed the feed horns; Glenn (Skip) Willman and his people, who manufactured many of the precisely machined parts making up the feed horns; Patrick Doherty and his crew, who did an excellent job manufacturing the antenna structure; Donald Brown and John Kangas, who performed innumerable bench tests on the multiple-beam antenna elements; Jeffrey Perry, Daniel Kane, and Frank Rittershaus, who constructed the four-channel nulling circuit used for performance testing and provided valuable assistance during the tests; David Besse, who wrote all the automated test programs and ensured that the test equipment was doing its job; and Theodore Arbo, Timothy Borge, John McCrillis, and Robert Piccola, who performed all the antenna range tests. A special acknowledgment goes to Robert Burns, who gave up his summer fishing seasons to coordinate people, places, and things, ensuring that the project ran smoothly from start to finish.

REFERENCES

1. S.P. Applebaum, "Adaptive Arrays," Syracuse University Research Corp., Report SPL TR 66-1, Aug. 1966.
2. R.A. Monzingo and T.W. Miller, *Introduction to Adaptive Arrays* (John Wiley, New York, 1980).
3. J.T. Mayhan, "Thinned Array Configurations for Use with Satellite-Based Adaptive Antennas," *IEEE Trans. Antennas Propag.* **8**, 846 (1980).
4. Electromagnetic Sciences, Inc., "Multibeam Lens Antenna for EHF SATCOM," Final Review, Contract F19628-86-C-0187, Electronic Systems Division, Air Force Systems Command (Sept. 1988).
5. A.J. Fenn, J.R. Johnson, L.W. Rispin, W.C. Cummings, and B.M. Potts, "High-Resolution Adaptive Nulling Performance for a Lightweight Agile EHF Multiple Beam Antenna," *MILCOM 91 Conf. Record,* vol. 2, p. 30.7.1, 1991.
6. Electromagnetic Sciences, Inc., "Lightweight EHF Beamforming Hardware for 7 Lens/127 Beam MBA," Final Report, Contract F19628-85-C-0002, prepared for MIT Lincoln Laboratory, 30 Mar. 1990.

WILLIAM C. CUMMINGS received his B.S. degree in electrical engineering from Northeastern University in 1958. From 1957 to 1961, he was a project engineer with Andrew Alford Consulting Engineers of Boston, where he designed special antennas for aircraft submarines and surface ships, television broadcast, and air navigation. In 1961 Bill joined Scanwell Laboratories of Springfield, Va., and became Vice President of Engineering in 1968. At Scanwell, he was responsible for the development of a variety of navigational and electronic countermeasure (ECM) antennas and related subsystems.

In 1971 he joined the staff of Adams-Russell Company of Waltham, Mass., where he directed the development of airborne high-power microwave antennas. From 1972 to 1977, he worked on shipboard communications antennas and navigational radar antennas as Vice President of Engineering at Eastern Microwave Corp. In 1977, Bill joined the Antennas Group of the Communications Division at Lincoln Laboratory. Since then, he has participated in studies relating to antenna beam-forming networks and autonomous adaptive antenna systems. He was a member of the team that provided technical support to the Military Satellite Communications (MILSATCOM) Systems Office of the Defense Communications Agency for the design of future MILSATCOM systems architecture. At Lincoln Laboratory, he became Assistant Group Leader of the Antennas Group in 1982 and Associate Group Leader of the Systems Engineering Group in 1987. He is currently Leader of the RF Technology Group.